# Effect of low intensity static magnetic field on purified water in stationary condition: ultraviolet absorbance & contact angle experimental studies

J.A. Dueñas,[1, a)] C. Weiland,[2] M.A. Núñez,[3] and F.J. Ruiz-Rodriguez[3]

[1)] *Departamento de Ingeniería Eléctrica y Centro de Estudios Avanzados en Física, Matemáticas y Computación. Universidad de Huelva, 21071 Huelva, Spain.*

[2)] *Departamento de Ciencias Agroforestales, ETSI Universidad de Huelva, 21071 Huelva, Spain.*

[3)] *Departamento de Ingeniería Eléctrica y Térmica, de Diseño y Proyectos, ETSI Universidad de Huelva, 21071 Huelva, Spain.*

(Dated: 3 March 2020)

This work focused its attention on the effect of low intensity static magnetic field on purified water: more specifically, on how the ultraviolet absorbance and the surface tension of the water may be affected. It has been found that pure water, exposed to a magnetic field for periods of time, does not absorb the ultraviolet radiation in an asymptotic way, but shows a local maximum at 15 minutes. It is also shown that the contact angle of droplets on paraffin can be reduced by up to 5 degrees by exposing the water to a 10 mT static magnetic field.

## I. INTRODUCTION

The physical and chemical properties of water have been, to some extent, changed by applying magnetic fields of different natures. Two main streams of interest regarding the exposure of water to an external magnetic field are producing a large number of works. The first deals with the study of the effect on the molecular structure of water by observing the change in dielectric constant, refractive index, volatility and surface tension among others properties[1–5]; these changes in the structure of water have been associated to hydrogen bonds.

The second stream is related to the study of the effect on the crystallisation of calcium carbonate $CaCO_3$, where the interaction of an external magnetic field with the charged species affects crystal nucleation and growth, mainly related to the scale prevention[6–11]. Furthermore, another distinction of these works may be made if we consider the kinetic condition of the water when the magnetic field is applied (i.e. circulating or static water), yielding a more complicated scenario since electric fields are induced by the passing of a conducting fluid through a magnetic field. The conductivity, the amount of evaporated water and the crystal formation have been reported to be affected by the flow rate[5,7,8].

Studies[12–15] of how a magnetic field interacts with hydrogen bonds have revealed a weakening effect in terms of breaking or reducing the number of hydrogen bonds. Hydrogen bond strength is about 23 kJ $mol^{-1}$ compare to the O−H covalent bond strength of 492 kJ $mol^{-1}$. It has been accepted that water molecule clusters may be classified according to the hydrogen bonds into inter- and intra-cluster. Simulations[15] have shown that a magnetic field can break the intra-cluster hydrogen bonds and strengthen the inter-cluster. Moreover, it has been reported[16] that the distribution of hydrogen bonds can be affected by the water's magnetic moment interaction in a magnetic field. Therefore, an external magnetic field can weaken, or even break, the hydrogen bonds, increasing the number of monomer water molecules.

Another classification of water molecules can be categorized according to the two possible spin orientations of its hydrogen atoms so water is a mixture of two isomers that differ in the direction of their hydrogen spins: the spins are parallel in "ortho" water and antiparallel in "para" water. The spin isomers of water can be separated[17,18] but it is difficult to study their properties in bulk water so what is needed, therefore, is a way to observe just a single water molecule and to somehow control its isomerisation between the ortho and para forms. A procedure has been reported[18] in which researchers shot a slow beam of water molecules through an hexapole magnetic field assembly (strong magnetic field gradients); the field acted like a selective lens for ortho water, which, unlike para water, is sensitive to a magnetic field. Most recently[19] a water molecule has been encapsulated in a fullerene ($H_2O@C_{60}$) and shown that its bulk dielectric constant depends on the spin isomer composition.

On the whole, except for a few works, the static magnetic fields employed to magnetize the water were generally well above 200 mT, leaving the effects of low intensity field undetermined. To detect the changes produced by magnetic field ranging from 10 mT to 200 mT on purified water, we resort to photoelectron spectroscopy to assess the electronic transitions (ultraviolet region) by employing a commercial spectrophotometer. The authors employed wetting, which involves the measurement of contact angles, to study how a magnetic field changes the physical properties of water. In this work, a direct optical method for measuring the contact angle was employed because of its simplicity, i.e. requires small droplets, no elements between the camera and the droplet, and free online image processing software.

Water magnetic treatment is commonly consider to be a controversial process, and according to some authors the results of the experimental work has been primarily qualitative and unreliable. However, the methodology employed by the authors makes sure that the results are well founded on the whole and easily reproducible.

[a)] Electronic mail: jose.duenas@die.uhu.es

## II. MATERIALS AND METHODS

### A. Static magnetic field generator

A homemade static magnetic field generator was assembled by wrapping three coils around a hollow rectangular iron core (cross-section $25 \times 25$ mm$^2$) with a narrow air gap of 15 mm, see inset in Fig. 1(a). The copper coils (wire of 1.2 mm in diameter) form a series circuit, which is connected to a direct current (DC) variable source, capable of supplying up to 5 A. To measure the magnetic field at the gap, a Gaussmeter GM08 manufactured by Hirst Magnetic Instruments Ltd was employed. The magnetic hysteresis loop of our system is shown in Fig. 1(a), where the experimental values (symbols) were obtained by increasing the current up to 5 A (upward) and then reducing the current back (downward). The residual magnetism is $\pm 7$ mT, which limits the lowest value of the magnetic field generator for a current sign. The versatility of the system allows a controllable working range from above 7 mT up to 200 mT. Stability tests were performed to ensure that the magnetic field at the gap did not fluctuate out of the GM08 precision range (0.1 mT) over time. A magnetic field cross-section plot can be seen at Fig. 1(b), where the maximum value of the field is found at the central area, about 2 cm $\times$ 2 cm.

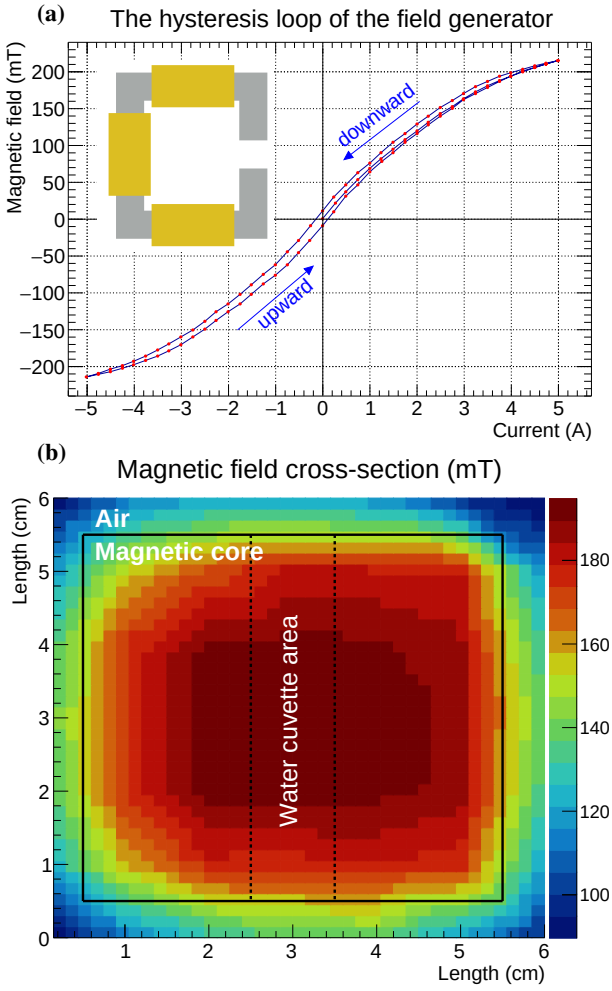


FIG. 1. (a), static magnetic field values vs applied risen (up) and fallen (down) current values, hysteresis loop. The inset shows a sketch of the homemade magnetic field generator consisting of a iron core with an air gap and three coper coils. (b), magnetic field cross-section obtained at the middle of the air gap for an applied current of 5 A.

### B. Sample preparation

High-level purified water (18.2 MΩ·cm at 298 K) produced by a Milli-Q Millipore System (Milli-Q Advantage A10) was employed. A volume of 1.3 mL of purified water is required to fill the microchannel of an ultraviolet quartz cuvette (10 mm path length) placed into the gap of the magnetic field generator, being the water volume completely exposed to the magnetic flux. Before placing the sample container, the magnetic field at the gap was always measured at the central area. Both the time and the static magnetic field to which the samples were exposed are given in following sections. It has to be mentioned that the volume of purified water, from which the samples were taken, was exposed to air over an hour to absorb atmospheric $CO_2$ and gases i.e. let the water fully equilibrate with air before using it.

### C. Spectrophotometer

An Agilent Cary 60 UV-Vis spectrophotometer was employed to perform absorbance studies in the ultraviolet (UV) region. The spectral resolution of the system is 1.5 nm with a focused beam measuring 1.5 mm $\times$ 1.0 mm. The Cary 60 system has incorporated a Peltier ($1 \times 1$) cell holder to control the sample temperature, which was set to match that of the purified water, room temperature. It has to be mentioned that all the system involved in the sample preparation, named the Milli-Q system and the magnetic field generator, where just a few meters away from the spectrophotometer and in the same room. The UV range studied was between 192 nm and 230 nm. The data was recorded with an interval of 0.15 nm and exported as a comma-separated values (CSV) file for data processing.

### D. Methodology and data processing

Figure 2 shows a block diagram of the procedure followed to measure the absorbance. The purified water was allowed to sit for one hour in a shallow dish before preparing the 1.3 mL sample (step 1). Then, the sample is placed in the spectrophotometer to obtain its UV spectrum (step 2). Next, the sample is taken to the magnetic field generator where it will be exposed to a given magnetic field for a period of time (step 3). Finally, the magnetized sample is placed in the spectrophotometer to once again obtain its UV spectrum (step 4). A few seconds passed between exposure and measurement. The instrument takes about 15 seconds to obtain the UV spectrum.

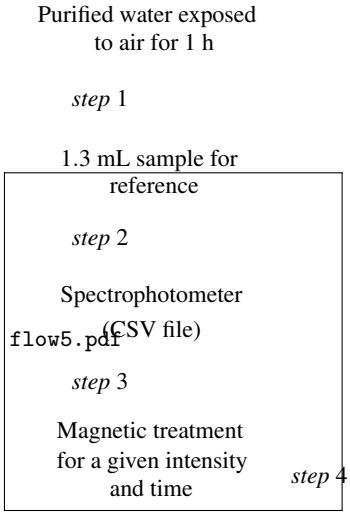


FIG. 2. Block diagram of the procedure followed to measure the absorbance of a magnetized sample and its reference sample.

Since the data were collected over time in different room conditions (i.e. lab without a controlled environment: atmospheric pressure, humidity, etc.), and in order to be able to study the relative amount of light that was absorbed by the samples as a function of both the applied magnetic field and exposure time $A_R(B,t)$, the following formulas were employed:

$$A_R(B,t) = \bar{A}_R(B,t) \pm \sigma_{A_R} \tag{1}$$

$$\bar{A}_R(B,t) = \frac{100}{5}\sum_{i=1}^{5}\frac{A_{M_i}(B,t) - A_{0_i}}{A_{0_i}} \tag{2}$$

$$\sigma_{A_R} = \sqrt{\left(\frac{\partial A_R}{\partial A_M}\right)^2 \sigma_{A_M} + \left(\frac{\partial A_R}{\partial A_0}\right)^2 \sigma_{A_0}} \tag{3}$$

where $A_{M_i}(B,t)$ is the absorbance of the sample $i$ after being exposed to a given magnetic field ($B$) for a given time ($t$), and $A_{0_i}$ is the absorbance of the sample $i$ before the magnetic treatment i.e. reference sample. To ensure reproducible and reliable measurement, the average relative absorbance $\bar{A}_R(B,t)$ was calculated out of 5 samples i.e. 5 spectra were taken from samples before, and another 5 spectra after the magnetic treatment. The formula is multiplied by 100 to express it in percentage. The variance of the relative absorbance $\sigma_{A_R}$ is calculated by error propagation employing the standard deviation of the spectra before ($\sigma_{A_0}$) and after ($\sigma_{A_M}$) magnetic treatment. The values of $B$ and $t$ employed are shown in the following result section.

### E. Contact angle measurements

Purified water was applied as 1 $\mu$L droplets using a microsyringe and micro-applicator on a plastic paraffin film placed on a spruce square rod. The contact angle was defined as the angle formed by the intersection of the water-surface interface and the water-air interface (tangent to the droplet profile). By employing a high-definition camera with macro objective coupled up to a microscope (Leica MZ6), a picture of each droplet was taken after 20 seconds of deposition. To accurately measure the contact angle of each droplet we employed an image processing software ImageJ 1.48 V[20]. A total of 30 droplets (sample size $n = 30$), for each magnetic treatment, were employed to obtain the contact angle mean value ($\bar{\theta}_{ca}$) and also the sample standard deviation ($s$). Then, the standard error of the mean ($\sigma_{\bar{\theta}_{ca}}$) was estimated as the sample standard deviation divided by the squared root of the sample size ($\sigma_{\bar{\theta}_{ca}} = s/\sqrt{n}$).

## III. RESULTS AND DISCUSSION

### A. Ultraviolet absorbance

The absorbance spectra of purified water under the influence of a magnetic field of 200 mT, for different magnetization times (i.e. the time to which the sample was exposed to the field), can be seen in Fig. 3(a). For the sake of clarity, the results shown in pad (a) are from single measurements (one spectrum per magnetization time), as explained previously the statistics are built on five samples per variable (i.e. magnetization time or magnetic field strength). In general, the absorbance increased with the magnetization time going from the bottom dashed curve, which corresponds to no magnetized water or no applied field, to the top curve obtained after the sample was exposed to a magnetic field of 200 mT for 15 minutes. Differences between two adjacent curves were not well distinguished with the naked eye; however, the separation is easily observed when comparing the spectra of a given magnetized sample with the no magnetized sample. Moreover, a clearer quantification for these differences can be made by obtaining the relative absorbance as explained in the methodology and data processing section shown in Fig 3(b). Here, the relative absorbance for an applied field of 200 mT reaches nearly 8% for a magnetization time of 15 minutes (upper spectrum), and even after just 2 minutes most of the wavelengths exceeded a value of 2% (lower spectrum). Similarly, in Fig. 3(c) the relative absorbance as a function of the applied magnetic field, for a magnetization time of 15 minutes, yields values of about 2% for 10 mT and up to 6% for 150 mT.

From Fig. 3 the conclusion could be easily drawn that both the magnetization time and the magnetic field intensity would have the same effect on the UV spectra of purified water i.e. the longer the magnetization time the higher the absorbance or as the magnetic field increases so does the absorbance. However, it has been found that for magnetization time greater than 15 minutes, the absorbance is no longer rising but falling, as shown in Fig. 3(d), where the values are shown of the relative absorbance at a wavelength of 200 nm as a function of the magnetization time for different applied magnetic fields. The value of 380 mT was obtained by employing a sandwich structure of two Neodymium magnets, confirming once again the

maximum value at 15 minutes. This "peak behaviour" contrasts with the expected asymptotic profile, i.e. absorbance increases until it approaches some fixed value of magnetization time, at which point it levels off, otherwise found by[3,21] in the infrared region of 4400-6000 $cm^{-1}$. Nevertheless, in agreement with the latter references, it has been found a linear relation between the absorbance (regardless of the difference in the studied wavelength regions) and the intensity of the applied magnetic field: that is, that the absorbance increases with increasing magnetic field. However, the experiments performed in this work did not show any "saturation effect" or asymptotic behaviour within our 30 minutes' magnetization time, which was the time window to ensure a temperature variation less than one degree Celsius. Experiments were carried out by varying the Peltier temperature of the spectrophotometer to verify that the UV spectrum of untreated purified water sample was not affected by a two degrees Celsius increment.

Two more experiments were performed to attain the restoration of the absorbance value after magnetization. The first consisted in extending the magnetization time well beyond the found local maximum as shown in Fig. 4. For one hour of treatment the relative absorbance (at 200 nm) is about 1% i.e. water still being affected by the magnetic field and was not fully restored to its original state. The second experiment dealt with residual magnetism. A sample was magnetized for 15 minutes with a field of 150 mT, then the spectrophotometer was set to obtain the absorbance spectrum in intervals of 15 minutes for 18 hours i.e. a total of 72 spectra to assess the relaxation time. The temperature was kept constant by the Peltier device. After this period no significant difference was fount i.e. the absorbance values were barely unaltered throughout the UV range. This phenomenon of "memory" of magnetized water, which as proved it is a function of not only the intensity of the applied field but also of the magnetization time, has also been reported[5,7] to last from 24 h up to 200 h.

As far as the authors know, this is the first experimental evidence of the absorbance peak behaviour with magnetization time in the UV region under study. However, references have been found[15,16] where computer simulation works show that the relationships between the internal energy, the heat capacity of water, and the external magnetic field strength are multipeak functions not an asymptotic. They conclude that an external magnetic field weakens the hydrogen bonds intra clusters, breaking the larger clusters, forming smaller clusters. This readjustment of molecules and their polarization distribution will increase the nonbonding electrons susceptible to transitions, and therefore the UV absorbance will increase. An externally applied magnetic field enhances the UV absorption of purified water. In our case, the fact of having an increasing absorbance reveals the time needed to optimize the process of weakening the hydrogen bonds and therefore the subdivisions of the clusters. With the application of a magnetic field the UV absorbance researches its maximum value after 15 minutes Fig. 3(d). Continuing the application of the magnetic field does not lead to an increase in UV absorbance; rather, it diminished it in proportion to the time the magnetic field is applied Fig. 4. By increasing the magnetization time the effect on the water clusters is reversed, reducing then the non-

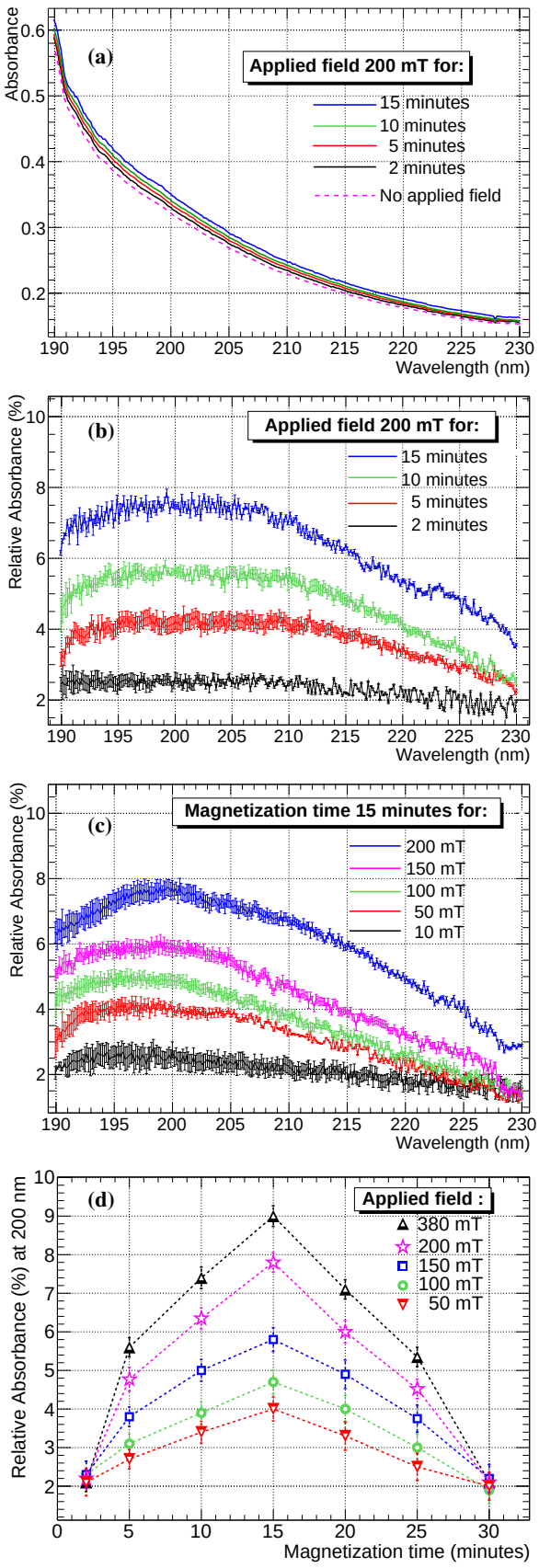


FIG. 3. The absorbance (a) and relative absorbance (b) spectra of purified water for different magnetization time. Relative absorbance for different applied magnetic fields (c). Relative absorbance at 200 nm vs time (d).

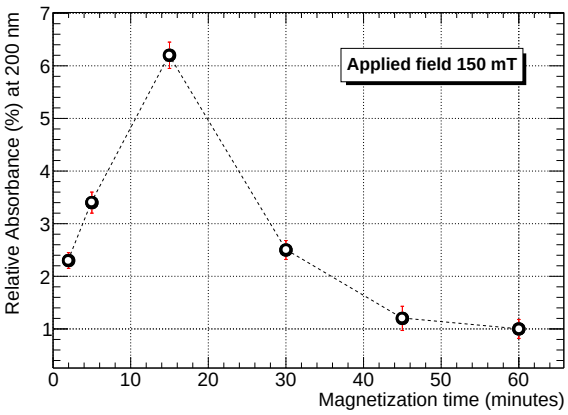


FIG. 4. Relative absorbance at 200 nm vs magnetization time for an applied field of 150 mT. After 1 h of treatment the absorbance gets closer to the sample pretreatment state.

bonding electrons and causing a drop in absorbance. Authors believe that this local maximum could be shifted for other different forms of water or under extreme conditions e.g. temperature and pressure, which will be a subject for future work.

Considering recent research on ortho and para water[22,23] and the fact that the ortho component interacts with an external magnetic field, it seems plausible that the process of weakening and breaking are mostly induced in hydrogen bonded cluster formed by ortho water molecules, which in turn may be an advantage when separating these two spin isomers. The ortho:para ratio is 3 : 1 at room temperature and its equilibrium takes nearly an hour[24]. However, recent works[25] set this ratio closer to 1 : 1 in liquid water due to hydrogen bond formation, and one would expect a shorter time to reach it. Our local maximum found at 15 minutes of magnetization time may be a indicator of it.

### B. Contact angle

Two examples of 1 $\mu$L droplets are shown in Fig. 5(a) and (b). The image processing software calculated the contact angles employing both the sphere and the ellipse approximations, Fig. 5(a') and (b') respectively. The final value of the contact angle was the average of both the right and left contact angles of the droplet. The results obtained from the study of the influence of the magnitezation time on the contact angle are shown in Fig. 6(a), where the applied magnetic field was changed from 10 mT to 200 mT. Similarly, the results obtained from the study of the influence of the magnetic field strength on the contact angle are shown in Fig. 6(b), where three data sets corresponding to samples magnetized in different days, for a magnetization time of 15 minutes, are shown. The experimental contact angles are given by the mean (solid symbol) and its standard error (error bars), $\bar{\theta}_{ca} \pm \sigma_{\bar{\theta}_{ca}}$. The tendency curves (dotted lines in Fig. 6) are obtained by fitting the experimental data with the following equation:

$$\theta_{ca}(x) = \theta_{asym}(1 + A_0\, e^{-\alpha x}) \qquad (4)$$

where $\theta_{asym}$ is the angle at which the plateau ends up (asymptotic value) and $\alpha$ governs how fast it gets there (decay rate); the constant $A_0$ yields the contact angle before magnetic treatment, $\bar{\theta}_{ca}(0)$. Table I shows the parameter employed to produce the tendency curves in Fig. 6(a) i.e. the calculated contact angle as a function of the magnetization time $\theta_{ca}(t)$;

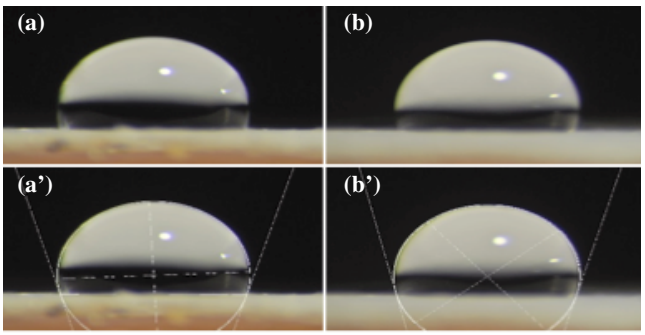


FIG. 5. Photographs of two different 1 $\mu$L droplets (a) and (b). The image processing software estimates the contact angles following the fitting lines (a') and (b'). 30 photographs are taken for each magnetic treatment.

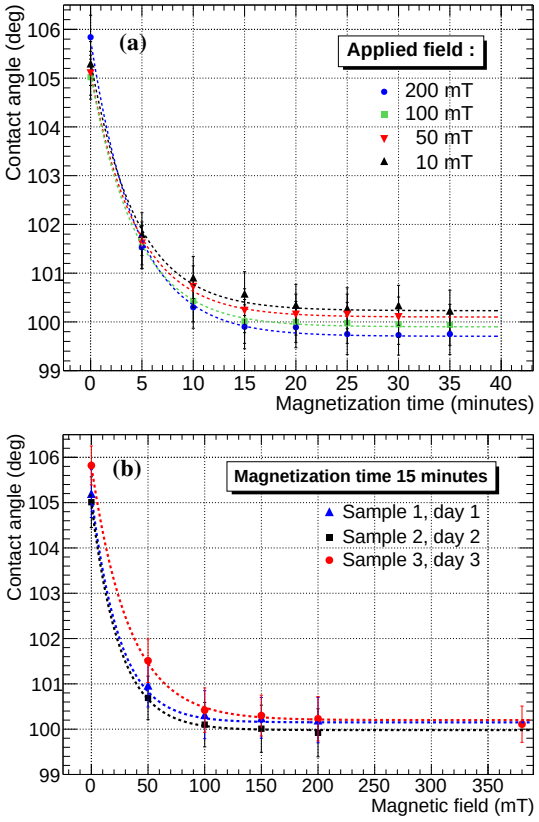


FIG. 6. Contact angle as a function of the magnetization time for different applied magnetic fields (a), and as a function of the magnetic field strength for a magnetization time of 15 minutes (b). Dotted curves show the central tendency of the contact angle according to eq. 4.

and table II shows the ones to produce the tendency curves in Fig. 6(b) i.e. the calculated contact angle as a function of the applied magnetic field $\theta_{ca}(B)$.

TABLE I. Parameters to produce tendency curves in Fig. 6(a). See text for parameter definition.

| Data set | $\bar{\theta}_{ca}(0)$ | $\theta_{asym}$ | $A_0$ | $\alpha$ |
|---|---|---|---|---|
| ▲ 10 mT | 105.1 | 100.230 | 0.051 | 0.225 |
| ▼ 50 mT | 105.3 | 100.101 | 0.050 | 0.225 |
| ■ 100 mT | 105.0 | 99.899 | 0.052 | 0.225 |
| ● 200 mT | 105.8 | 99.705 | 0.061 | 0.225 |

TABLE II. Parameters to produce tendency curves in Fig. 6(b). See text for parameter definition.

| Data set | $\bar{\theta}_{ca}(0)$ | $\theta_{asym}$ | $A_0$ | $\alpha$ |
|---|---|---|---|---|
| ▲ Sample 1 | 105.2 | 100.15 | 0.050 | 0.040 |
| ■ Sample 2 | 105.0 | 99.98 | 0.050 | 0.040 |
| ● Sample 3 | 105.8 | 100.20 | 0.056 | 0.030 |

We carried out a control experiment to study the time evolution of the contact angle without the applied field. The results of which are shown in table III. Then, we produced four batches of droplets from the same purified water sample with ten minutes time difference, but we did not applied the magnetic field and found that the contact angle barely changed, proving that only the applied field caused the change in contact angle.

TABLE III. Average contact angle $\bar{\theta}_{ca}$ and its sigma $\sigma_{\bar{\theta}_{ca}}$ without applied field, time steps of 10 minutes.

| Time (minutes) | 0 | 10 | 20 | 30 |
|---|---|---|---|---|
| $\bar{\theta}_{ca}$ | 105.8 | 105.9 | 105.7 | 105.6 |
| $\sigma_{\bar{\theta}_{ca}}$ | 0.5 | 0.6 | 0.7 | 0.5 |

The overall conclusion of these experiments is that the contact angle, and therefore the surface tension forces, of the droplets are being affected by low intensity static magnetic fields. Moreover, from Fig. 6(a) it can be seen that the plateau is reached for a magnetization time of roughly 15 minutes or longer, which coincides with the relative absorbance peak shown in Fig 3(d). These findings have revealed that the maximum effect of an applied static magnetic field, on the ultraviolet absorbance and on the contact angle, happens at magnetization time of about 15 minutes. Similar "plateau" behaviour, concerning the contact angle, has been reported in[26,27] although no detailed values of magnetization time or applied magnetic field are given. Figure 6(b) also reveals that, for a magnetization time of 15 minutes, the contact angle reaches an asymptotic value above 50 mT; the experiment was repeated in three different days, employing on day 3 the Neodymium magnets to reach the 380 mT. The contact angles measured before magnetic treatment $\bar{\theta}_{ca}(0)$ are within the expected range since pure water droplet makes a contact angle of 105° to 110° with a smooth paraffin surface[28]. As shown in table I, the original contact angle $\bar{\theta}_{ca}(0)$ has been reduced up to 5 degrees, which means that the spreadability or wettability has been increased. It is known that the reduction of the contact angle of magnetized water is due to the increase of polarized effect and the changes of distribution and clustering structure of water molecules after magnetization[29,30].

## IV. CONCLUSIONS AND FUTURE WORKS

The experiments carried out during this work have shown that a static magnetic field of just 10 mT, applied to a volume of 1.3 mL of purified water, increases the absorbance of the UV spectrum in the region of 190 to 230 nm. It was also shown that the relative absorbance as a function of the magnetization time is not asymptotic, but presents a local maximum at 15 minutes, which is the time required for the stabilization of nonbonding electrons. Furthermore, the contact angle of purified water droplets on paraffin film was reduced by 5 degrees after a magnetization time of 15 minutes, employing a 10 mT magnetic field. In this study, the contact angle as a function of both the magnetization time and the applied field showed a plateau behaviour, which is in agreement with other authors. The authors plan, in the near future, experiments to look further into the studied effects, but employing a pulsed magnetic field i.e. short but strong pulse of magnetic field, and to develop some new theoretical models.

## ACKNOWLEDGMENTS

This work was supported in part by the Sistema Nacional de Garantía Juvenil and Programa Operativo de Empleo Juvenil (Grant code SNGJ-JPI-075). The authors wish to thanks the Laboratorio de Investigación y Control Agroalimentario de Huelva (LICAH- Edificio CIDERTA) of Huelva University for the use of the lab and equipment.

## REFERENCES

[1] M. Kiselev and K. Heinzinger, "Molecular dynamics simulation of a chloride ion in water under the influence of an external electric field," J. Chem. Phys **105**, 560 (1996).
[2] Y. Zhu, L. Yan, Z. Cao, L. We, and Z. Chen, "Physical and chemical properties of magnetized water," J Hunan Univ (Nat Sci) **26**, 21–26 (1999).
[3] B. Deng and X. Pang, "Variations of optic properties of water under action of static magnetic field," Chinese Science Bulleting **52**, 3179–3182 (2007).
[4] R. Cai, H. Yang, J. He, and W. Zhu, "The effects of magnetic fields on water molecular hydrogen bonds," J. Mol. Struct. **938**, 15–19 (2009).
[5] A. Szcześ, E. Chibowski, L. Holysz, and P. Rafalski, "Effects of static magnetic field on water at kinetic condition," Chem. Eng. Process. **50**, 124–127 (2011).
[6] Y. Wang, A. Babchin, L. Chernyi, R. Chow, and R. Sawatzky, "Rapid onset of calcium carbonate crystallization under the influence of a magnetic field," Wat. Res. **31**, 346–350 (1997).

[7] J. Coey and S. Cass, "Magnetic water treatment," J. Magn. Magn. Mater. **209**, 71–74 (2000).

[8] C. Gabrielli, R. Jaouhari, G. Maurin, and M. Keddam, "Magnetic water treartment for scale prevention," Wat. Res. **35**, 3249–3259 (2001).

[9] S. Kobe, G. Drazic, A. Cefalas, E. Sarantopoulou, and J. Strazisar, "Nucleation and crystallization of $CaCO_3$ in applied magnetic fields," Crystal Engineering **5**, 234–253 (2002).

[10] C. Tai, M. Chang, R. Shieh, and T. Chen, "Magnetic effects on crystal growth rate of calcite in a constant-composition environment," J. Cryst Growth **310**, 3690–3697 (2008).

[11] C. Tai, C. Wu, and M. Chang, "Effects of magnetic field on the crystallization of $CaCO_3$ using permanent magnets," Chem. Eng. Sci. **63**, 5606–5612 (2008).

[12] S. Maheshwary, N. Patel, N. Sathyamurthy, A. Kulkarni, and S. Gadre, "Structure and stability of water clusters ($h_2o$)(n), n=8 – 20: An ab initio investigation," J. Phys. Chem. A **105**, 10525–10537 (2001).

[13] N. Su and C. Wu, "Effect of magnetic field treated water on mortar and concrete containing fly ash," Cem. Concr. Compos. **25**, 681–688 (2003).

[14] R. Krems, "Breaking van der waals molecules with magnetic fields," Phys Rev. Lett. **93**, 13201 (2004).

[15] E. Toledo, T. Ramalho, and Z. Magriotis, "Influence of magnetic field on physical-chemical properties of the liquid water: insights from experimental and theoretical models," J. Mol. Struct. **888**, 409–425 (2008).

[16] K. Zhou, G. Lu, Q. Zhou, S. J. J.H. Song, and H. Xia, "Monte carlo simulation of liquid water in a magnetic field," Journal of Applied Physics **88**, 1802–1805 (2000).

[17] T. Kravchuk, M. Reznikov, P. Tichonov, N. Avidor, Y. Meir, A. Bekkerman, and G. Alexandrowicz, "A magnetically focused molecular beam of orthowater," Science **331**, 319–321 (2011).

[18] D. Horke, Y. Chang, K. Dlugolecki, and J. Kupper, "Separating para and ortho water," Angew. Chem. Int. Ed. **53**, 11965–11968 (2014).

[19] B. Meier, S. Mamone, M. Concistre, J. Alonso-Valdesueiro, A. Krachmalnicoff, R. Whitby, and M. Levitt, "Electrical detection of ortho-para conversion in fullerence-encapsulated water," Nature Commun. **6**, 8112 (2015).

[20] W. Rasband, "Imagej," U. S. National Institutes of Health, Bethesda, Maryland, USA , https://imagej.nih.gov/ij/, 1997–2016.

[21] X. F. Pang, "The experimental evidences of the magnetism of water by magnetic-field treatment," IEEE Transactions on Applied Superconductivity **24**, 4402806 (2014).

[22] S. M. Pershin, "Coincidence of rotational energy of $h_2o$ ortho-para molecules and translation energy near specific temperatures in water and ice," Phys. Wave Phenomena **16**, 15–25 (2008).

[23] S. D. Zakharov, "Ortho/para spin isomers of h2o molecules as a factor responsible for formation of two structural motifs in water," Biophysics **58**, 718–722 (2013).

[24] V. I. Tikhonov and A. A. Volkov, "Separation of water into its ortho and para isomers," Science **296**, 2363 (2002).

[25] S. M. Pershin, "Effect of quantum differences of ortho and para h2o spin-isomers on water properties: biophysical aspect," Biophysics **58**, 723–730 (2013).

[26] M. Amiri and A. Dadkhah, "On reduction in the surface tension of water due to magnetic treatment," Colloids Surf A: Physicochem Eng Aspects **278**, 252–255 (2006).

[27] Y. Cho and S. Lee, "Reduction in the surface tension of water due to physical water treatment for fouling control in heat exchangers," Int. Commun. Heat Mass Transfer **1**, 1–9 (2005).

[28] W. A. Zisman, "Relation of the equilibrium contact angle to liquid and solid constitution," Chapter **1**, 1–51 (DOI:10.1021/ba-1964-0043.ch001).

[29] k.T. Chang and C. Weng, "The effect of an external magnetic field on the structure of liquid water using molecular dynamics simulation," Journal of Applied Physics **100**, 043917–043922 (2006).

[30] X. Pang and B. Deng, "Investigation of changes in properties of water under the action of a magnetic field," Sci China Ser G-Phys Mech Astron **51**, 1621–1632 (2008).